

Performance Optimization of High-Altitude Platform Wireless Communication Network Exploiting TVWS Spectrums Based on Modified PSO

HABIB MOHAMMED HUSSEIN ¹, KONSTANTINOS KATZIS ² (Senior Member, IEEE),
LUZANGO PANGANI MFUPE ³ (Senior Member, IEEE),
AND EPHREM TESHALE BEKELE ¹ (Senior Member, IEEE)

¹Department of Electrical and Computer Engineering, Addis Ababa Institute of Technology, 1000 Addis Ababa, Ethiopia

²European University of Cyprus, 2404 Egkomi, Cyprus

³CSIR, 395 Pretoria, South Africa

CORRESPONDING AUTHOR: HABIB MOHAMMED HUSSEIN (e-mail: habib.mohammed@aait.edu.et)

ABSTRACT The Uniform hexagonal array (UHA) sidelobe level (SLL) reduction is a crucial consideration for avoiding co-channel interference and improving Carrier-to-interference Ratio (CIR) performance in HAP wireless networks using the TVWS spectrum. The SLL reduction in UHA has been researched by applying evolutionary algorithms such as genetic algorithm (GA) and Particle Swarm Optimization (PSO). However, such algorithms have the drawbacks such as early convergence and the inability to reach globally. The beam pointing approaches for UHA antennas using Modified PSO (MPSO), for reducing the SLL on finding the optimal current weights is presented in this article. The UHA antenna array with 19 cells fitted with 169 elements in the HAPs cellular structure is considered to simulate the proposed approach. Then, the MPSO approach is employed and compared with the standard PSO algorithm and Uniform Weighting (UW) scheme. As per the simulation findings, the proposed approach drastically decreased sidelobes, with a reduction of up to -6.84dB and -13.3dB when compared to PSO and UW respectively. In other words, the proposed approach outperforms the UW and the PSO algorithms. Moreover, the CIR performance of the proposed approach has been demonstrated in terms of average outage probability and the proposed approach provides a better result.

INDEX TERMS Antenna array, array factor, beam pattern, carrier to interference ratio, high altitude platform, sidelobe level, TVWS, uniform hexagonal array.

I. INTRODUCTION

In contemporary society, having access to the internet has been crucial in terms of improving various aspects of people's lives by giving far-reaching economic and social benefits. As a consequence, a profusion of wireless devices with novel capabilities that need a considerable amount of radio spectrum to operate is on the rise. According to the CISCO virtual network index, there will be 29.3 billion networked devices by 2023 [1] in the years 2018 to 2020. Smart devices with greater capability that need higher bit rates and storage, increasing video consumption, system proliferation, and

application acceptance are all factors that influence the growth of potential International Mobile Telecommunications (IMT) traffic [2]. Global monthly mobile data traffic is expected to reach 158EB in 2022 and 5016EB in 2030 [2].

Existing networks are being strained by the ever-increasing demand for bandwidth, as well as the introduction of new growing applications. The spectrum, on the other hand, is very difficult to meet this expanding demand and is a scarce resource. With the ever-increasing number of wireless devices on the market and the limiting amount of spectrum available, resource management has never been more important.

Various alternative technologies and methods, such as TV White Space (TVWS) with Cognitive Radio Networks (CRN) [3], Massive Multiple Input Multiple Output (MIMO) [4], Beamforming [5], High Altitude Platforms (HAPs) [6], Visible light communication [7], and so on, have been proposed over time to alleviate the spectrum burden. Despite this, a 2017 poll by the International Telecommunication Union (ITU) found that more than half of the world's population does not have access to the internet [8]. According to the poll, around 74% of Africans and 14% of Europeans do not have access to broadband since they live in rural and isolated areas. The percentage for Africa suggests that a large chunk of the continent is underserved. Broadband deployment in these remote areas will significantly increase their economies and raise their living standards. Ethiopian wireless telecommunications coverage is now centered mostly in urban and suburban areas. In Ethiopia, rural regions account for more than 80% of the population [9]. Unfortunately, in rural areas, terrestrial communication systems are commercially unviable due to unreasonably high deployment costs and low user density. The primary problems of rural connection are high network installation costs, sparse population density, concentrated settlements, intermittent/no energy supply, poor income, and so on [10]. It is critical to provide a robust and cheap internet infrastructure capable of connecting such a vast number of individuals and assisting them in improving their economic situation. In this context, developing technologies such as TVWS, the Global System for Mobile White Spaces (GSMWS), visible light communication [11], adoption of open/virtualized/cloud-native systems [12], and HAP [9], [10] and [13] may open up new options. According to studies [9], [10], and [13], using HAPs to supply telecommunications services is a financially feasible option.

HAPs are manned or unmanned aeronautical platforms that are used for wireless applications and are normally located between 17 and 22 kilometers in altitude. The authors of [9], [10], and [13] stress that better delivery of healthcare and educational services, community growth and small business expansion, prevention of rural-urban migration, and the interaction of communication infrastructure with different services are all common advantages of broadband penetration in rural nations. The literature referenced in [9], [10], and [13] proved the benefits of HAPs for overcoming specific wireless communication challenges over terrestrial wireless and satellite systems. The estimates appropriately represent the cost advantage of HAPs over terrestrial systems. A macrocell with a radius of 1 km is projected to cost about 168 000 euros (9.744 million Birr) to build, run, and maintain [9] and [10]. For a 30km radius of continuous coverage, at least 900 of these macrocells are needed. As a result, it is anticipated that the network would cost 151 million euros, or 8.758 billion Birr. Contrarily, an unmanned solar aircraft would cost around 5 million euros (290 million Birr) to deploy, operate, and maintain to cover the same service area, as stated in these articles. HAPs are inexpensive, easy to install, and may be utilized for a longer length of time than other types of covering. These traits indicate that HAPs are a viable solution

for rural wireless communication because they satisfy the requirements for a rural wireless communication system listed in [9] and [10]. In addition, HAPs offer enough coverage with fewer handovers over a regional service area, considerable capacity increases, better throughput, reduced latency, and an expanded link budget when compared to satellites. Because of their higher elevation angle, HAPs have a far greater coverage advantage than terrestrial systems. Since of the cheap cost of deployment, HAPs are particularly useful in both rural and urban regions because they can be incorporated into the networks of major mobile and broadband networks to provide high capacity and extended coverage wireless services [9], [10], [13] and [14]. The quality of HAP communications has recently been tested in situations including Worldwide Interoperability for Microwave Access (WiMAX) [14], 3G [15], 4G/Long-term Evolution (LTE) [16], 5G [17], and beyond 5G [18]. High-altitude balloons were used in Project Loon to bring Internet access and coverage to unserved and underserved regions [19]. The research proved that LTE from HAP using the 700MHz band is possible. Researchers from all around the globe are now investigating the feasibility of using the underutilized/unused section of the television spectrum called TVWS) to provide rural wireless internet. In [9], [13], [20]–[23], the notion of providing wireless internet from the HAP via the TVWS band is presented. HAPs and TVWS technologies, as are among the facilitators of Universal Internet Access as part of the 5G and beyond 5G ecosystem, according to the authors of [24]. Among the several favorable characteristics of HAPs discussed above, certain difficult issues remain unexplored at the moment. Among these challenges, radio coverage expansion, capacity enhancement, sidelobe reduction, and the antenna beam pointing optimization to construct ground cells are critical. The antenna technology utilized to establish communication with or from users inside cells is a critical and HAP crucial parameter. A solution has been provided in [25]–[28] using spot-beam antennas and array processing algorithms. This research is a continuation of the work in [9], [13], [21]–[23] and focuses on the effect of uniform hexagonal antenna arrays (UHA) on reducing the sidelobe level and optimizing the performance of TVWS exploitation from the HAP. Utilizing the TVWS wireless network from HAP through UHA is a unique concept that has not been investigated before, to the author's knowledge. The interference that interacts with the other co-channel cells must be minimized to enhance the proposed model. To do that, the sidelobe levels must be minimized in UHA's radiation pattern to boost the capacity of HAPs networks over TVWS Spectrum. Therefore, a further goal of this study is to construct an array feeding function that can be altered to reduce sidelobe levels by applying modified particle swarm optimization (MPSO) to the other cochannel cells of UHA in order to improve the carrier-to-interference ratio (CIR). The contribution of this article may be summarized as follows:

- We advocate for a unique form of HAPs that utilizes TVWS bands as a viable option for rural customers to access broadband networks through a steerable beam of UHA.

- In order to improve the performance of the suggested system, we discuss the use of optimization strategies for lowering sidelobe levels.
- To illustrate the impact of increasing the number of UHA elements to lower sidelobe levels and optimize the beam pattern via the proposed a novel MPSO algorithm.
- For 169 antenna elements per HAP antenna array, we examine the performance of the proposed model optimization performance is compared with uniform weighting (UW) and Particle Swarm Optimization (PSO) algorithms in terms of sidelobe levels and Average outage probability.

The remainder of the article is structured as follows: Section II presents related works; Section III presents the system model and description for the proposed system; UHA beamforming optimization via MPSO is presented in Section IV; then, simulation results and description are illustrated in Section V; finally, Section VI concludes the article.

II. RELATED WORKS

Lately exploiting the TVWS spectrum from HAP is attracting a lot of interest in bridging the connectivity gap between rural and urban areas for the next generation of 5G wireless communications systems [9], [13], [21]–[23] and [29]. Due to the small space and weight of a HAP, the HAP antenna makes up a large portion of the payload, so developing the antenna with optimized parameters is critical [30]. One of the latest technologies for the deployment of HAP-based communication systems is smart antenna technology [31]. Smart antennas may generate several narrow beams that concentrate energy on restricted areas (cells). Smart antennas are good at interference suppressing capability so as to eliminate co-channel interference, thereby improving transmission efficiency as well as reducing transmitting power. In the area of wireless networking, one of the most recent developments to address the issue of rising demand for power is the implementation of a smart antenna or phased array antenna [32]–[34]. Among the types of phased array antennas, linear, circular, hexagonal arrays, and so on, are the most common ones. The linear array has a high degree of directivity and is capable of generating a narrow main lobe in a particular azimuth direction, albeit it does not perform well in all azimuth directions. Due to the absence of edge components in the circular array, directed patterns formed with it may be electrically rotated in the array's plane without materially altering the form of the beam [33]. However, the circular array pattern has no nulls in the azimuth plane, while the array pattern for smart antenna implementations can include multiple zeros in the azimuth plane to exclude Signals-Not-of-Interest (SNOI). Concentric arrays are used in [35] to lower side-lobe levels. Literature in [36] introduces the notion of using hexagonal antenna arrays for wireless communication. The superiority of hexagonal arrays over circular arrays was mentioned in [34]. Antennas serving cells produce interference in a HAPs system by intersecting the main lobes or sidelobes [37]. In fact, the array performance in terms of radiation pattern, gain,

beam steering, peak sidelobe level (PSLL), antenna mutual coupling, and inter-element distance significantly influences the quality of overall wireless communication [29]. When there are connections to line-of-sight (LoS), the CIR in a HAP cellular system is determined by the antenna radiation pattern. The higher the CIR value, the more capacity the device would have and the more additional services it will be able to provide. HAPs may use a variety of antenna configurations. Literature in [38] uses several aperture antennas in order to achieve a single spot beam per cell. Despite the great system capacity provided by HAP's low sidelobe levels, the antenna size and weight may be too big and unsuitable. The antenna array improves directivity and enables the detection of users on the ground through beamforming. A number of examples of antenna arrays for mm-wave communication are provided in reference [39]. In Reference [40], a 64 element (8x8) phased array operating at 28 GHz is described. Reference [41] illustrates a multi-beam lens antenna for a HAPS operating in the L/S band. Anokiwave presented a Ka-band phased array with a 4-channel beamformer circuit and 256 open-ended, substrate-integrated square waveguides in Reference [42]. Recently, it has been researched how to analyze the planar array antenna by reducing the maximum side lobe level (SLL) by optimizing the element spacing or excitation weights using genetic algorithms (GAs) [43] and particle swarm optimizer (PSO) [44]. Another approach was used in [45] to suppress the highest SLL with a certain half-power beamwidth. This approach was based on the improved discrete cuckoo search algorithm (IDCSA). However, the algorithm works by turning off specific array items. A Symbiotic Organisms Search (SOS) method was employed to reduce sidelobes in [46]. The SOS algorithm, unlike other techniques, has no tuning parameters, making it an appealing optimization approach. In these investigations, the PSO method performed better than other evolutionary algorithms. Early convergence is a major flaw in the classic PSO technique, particularly for multimodal situations. To increase the PSO's performance while dealing with multimodal situations, many PSO methods have been developed. An optimization approach that does not become stuck in a local optimum is required. Literature in [47], demonstrated that minimum sidelobe level can be obtained by using Ant Colony optimization. However, the algorithm faces a similar problem. This article aimed at optimizing the UHA beam pattern so as to point the beams to the desired location and reduce the sidelobe level thereby improving the performance of the HAP communication network by exploiting the TVWS spectrum using an MPSO. The article demonstrates how a UHA of uniformly stimulated isotropic antennas may be utilized to generate a directed beam with the lowest SLL. Optimizing the beam pattern of UHA thereby reducing SLL for HAP wireless communication system exploiting TVWS spectrum using MPSO algorithm has never been attempted before to the author's knowledge and is the focus of this article. The proposed approach then improves system performance by improving the CIR value.

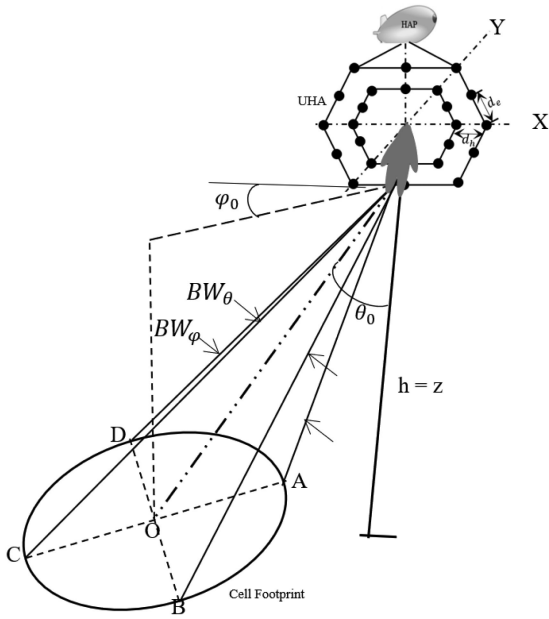


FIGURE 1. UHA system with cell footprint for HAP utilizing TVWS.

III. SYSTEM MODEL AND DESCRIPTION

A scenario of HAP downlink communications in the TVWS band is considered, where the platform is located at an altitude of 20 km. The scenario takes into account a 10.5 kilometer cell radius and a 100 km coverage radius. As shown in Fig. 1 below, a payload of 19 TVWS base stations outfitted with a 169 element UHA antenna is taken into consideration for beamforming and delivering HAP beams. We used UHA in this study. Mobile network cells are built by directing beams from HAP that is situated at a height of around 20 kilometers above the ground. In phased array design, a $\lambda/2$ maximum separation is assumed between the antenna elements to eliminate the grating lobes in the antenna gain pattern.

For every user on the ground, a beam's footprint has a pointing direction of (θ_0, φ_0) , a cross-section half-power beamwidth (HPBW) of BW_θ, BW_φ and an approximate ellipse-shaped beam projection on the ground as illustrated in Fig. 1 [34] and [36]. The array factor (AF) for the hexagonal array is given by

$$AF(\theta_0, \varphi_0) = \sum_{m=0}^{M-1} A_m e^{jkr_{1m} \sin\theta (\cos\varphi_{1n} \cos\varphi + \sin\varphi_{1n} \sin\varphi)} \times \sum_{n=0}^{N-1} B_n e^{jkr_{2n} \sin\theta (\cos\varphi_{2n} \cos\varphi + \sin\varphi_{2n} \sin\varphi)} \quad (1)$$

The value of r_1 and r_2 can be obtained as follows using Fig. 2 below, where $r_2 = r_1 \cos(\pi/N)$, $r_1 = de / \sin(\pi/N)$, along the sides of the UHA, there is an inter-element spacing de , $\phi_{1n} = 2\pi(n-1)/N$ denotes the angle in xy plane for n^{th} element at vertices of a hexagon, the angle in the xy plane for the x -axis and the n^{th} element at the hexagon's

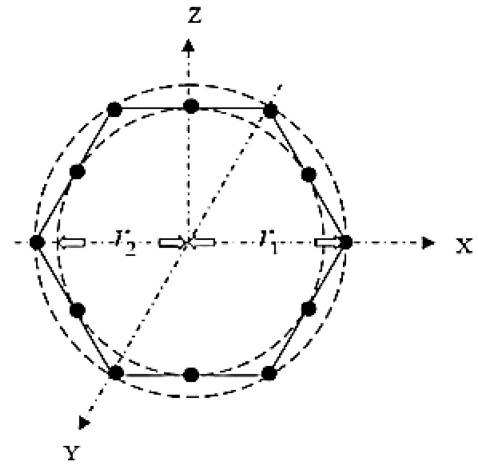


FIGURE 2. Uniform hexagonal array (UHA).

vertices is represented by $\phi_{1n} = 2\pi(n-1)/N$, the angle between the x -axis and the n^{th} element axis in the xy plane is denoted by $\phi_{2n} = \phi_{1n} + \pi/N$ at each hexagonal line's middle element, the amplitudes of the m^{th} element located at the vertices and center of the hexagon is represented by A_m and B_n .

IV. OPTIMIZING UNIFORM HEXAGONAL ARRAY ANTENNA BEAMFORMING VIA MODIFIED PSO

The PSO proposal was made by Eberhart and Kennedy in 1995 as an evolutionary computing strategy originated from the observation of bird predation activity [48]. PSO generates a collection of random solutions (initial swarm). Based on a tremendous amount of data about the design space that is absorbed and exchanged by all swarm members, this swarm is deployed over the design space in search of the best solution across a number of iterations (moves). A group of particles (solutions) that each have two vectors attached to them—a position vector, X_i , and a velocity vector, V_i represent the swarm in PSO.

The location of particle i in N -dimensional space is denoted by the vector, $X_i = (x_1, x_2, \dots, x_N)$, and the flight velocity is denoted by the vector, $V_i = (V_1, V_2, \dots, V_N)$. Each particle has a fitness value set by the objective function and is aware of its previous best position (p_{best}) and present position X_i . This may be seen as the particle's direct experience of flight. Additionally, each particle is aware of the best location (g_{best}) discovered so far by all particles in the group (g_{best} is the best value in p_{best}), which may be viewed as the particle companion's experience. Particles select their future journey based on their own experience and the best experience of their friends. After calculating these two ideal values, the particle uses the formula below to update its speed and position.

$$V_{i,k+1} = w * V_{i,k} + C_1 * rand_1 * (p_{best_{i,k}} - S_{i,k}) + C_2 * rand_2 * (g_{best_k} - S_{i,k}) \quad (2)$$

In (2), $V_{i,k}$ is the i^{th} particle velocity at the k^{th} iteration; w is weighting function; C_1 and C_2 are positive weighting factors; $rand_1$ and $rand_2$ are random numbers between 0 and 1; $S_{i,k}$ is i^{th} particle current position at the k^{th} iteration; $p_{best_{i,k}}$ is i^{th} particle personal best at the k^{th} iteration; g_{best_k} is best of the group at the k^{th} iteration. The following equation is used to modify the solution domain's search point.

$$S_{i,k+1} = S_{i,k} + V_{i,k+1} \quad (3)$$

The PSO is commonly used in many areas, including feature optimization, image processing, geodesy, and so on, due to its easy operation and rapid convergence speed. With the increase of the PSO algorithm's application range, difficulties such as premature convergence and a predisposition for slipping into local extreme value difficulties must be addressed. The following adjustments are made to the PSO's global search capabilities in order to address these issues. MPSO is the name given to this modified PSO [49]. The modified velocity of j^{th} component on i^{th} particle is expressed as follows:

$$V_{i,k+1} = r_2 * \zeta(r_3) * V_{i,k} + (1-r_2) * C_1 * r_1 * \{p_{best_{i,k}} - S_{i,k}\} + (1-r_2) * C_2 * (1-r_1) * \{g_{best_{i,k}} - S_{i,k}\} \quad (4)$$

In (4), C_1 and C_2 are the weighting coefficients that are used to control obtained results of each term. Because the main goal is to get the lowest possible SLL, the value of, C_1 is greater than the value of C_2 and r_1 , r_2 and r_3 are the random numbers between 0 and 1. The value of $\zeta(r_3)$ is using a function defined as follows:

$$\zeta(r_3) = \begin{cases} -1, & r_3 \leq 0.05 \\ 1, & r_3 > 0.05 \end{cases} \quad (5)$$

Personal and social experiences can be considered an unnecessary extravagance if they are made large enough to go beyond the optimum that has been reached locally. If both are modest, both personal and social experiences are underused, resulting in slower convergence of the approach. Following the definition of the UHA, the design approach proceeds to the formulation of the cost/fitness function in order to decrease the maximum SLL. As stated below, the fitness function formulation is done using signal to interference plus noise ratio (SINR). The SINR is described as the ratio of desired and undesired signal power [50] and [51].

$$SINR = P_{desired}/P_{undesired} = \alpha^2 |\bar{w}^H \bar{x}_s|^2 / \bar{w}^H \bar{R}_{uu} \bar{w} \quad (6)$$

In (6), \bar{w} is the complex array weight that can be obtained as $\bar{w} = \{w_{mn} e^{j\beta_{mn}}; m = 1, 2, \dots, M; n = 1, 2, \dots, N\}$ the amplitude and phase of the mn^{th} element is w_{mn} is the amplitude of mn^{th} element, and β_{mn} is phase of mn^{th} element, \bar{w}^H is complex array weight transpose, \bar{x}_s is a vector that describes the uniform hexagonal array's array factor, as discussed in the previous section. \bar{R}_{uu} is the undesired correlation matrix. \bar{R}_{uu} can be described by

$$\bar{R}_{uu} = \bar{R}_{ii} + \bar{R}_{nn} \quad (7)$$

In (7), \bar{R}_{ii} and \bar{R}_{nn} denotes a correlation matrix for interferers noise respectively.

For optimizing SINR, Applebaum optimization criterion [52] is applied. However, it is impossible to maximize the SINR in (6) directly, since neither α nor \bar{R}_{uu} is known or explicitly measured. Therefore, the fitness function $f(\bar{w})$ can be maximized by recasting (6) as follows

$$f(\bar{w}) = |\bar{w}^H \bar{x}_s|^2 / \bar{w}^H \bar{R}_{xx} \bar{w} \quad (8)$$

In (8), \bar{R}_{xx} is the array correlation matrix for the received signal. \bar{R}_{xx} can be obtained as

$$\bar{R}_{xx} = \bar{R}_{uu} + \bar{R}_{ss} \quad (9)$$

In (9), \bar{R}_{ss} is the desired signal correlation matrix. Correspondingly, the proposed population-based optimization algorithms will use (8) as the fitness function.

A. OUTAGE PROBABILITY

The degree of disturbance in a cellular system at any given moment is unpredictable, and it must be simulated by simulating both the RF propagation environment between cells and the mobile users' position. The CIR of the communication link is specified as the ratio of the desired signal to total interference signal power. CIR can be used to estimate the effects of co-channel interference. The CIR is therefore a random variable and all of these power levels are random variables due to RF propagation impact, user mobility, and traffic variation. As a result, the impact of co-channel interference on system performance is commonly stated in terms of system outage probability, which is defined as the chance that CIR falls below a certain threshold, CIR_{thresh} [53]. This is

$$P_{outage} = P_r [CIR < CIR_{thresh}] = \int_0^{CIR_{thresh}} pCIR(x) dx \quad (10)$$

In (10), $pCIR(x)$ is the probability density function (pdf) of the CIR and $CIR = \text{Desired power}/\text{Total interfering power}$.

UW: UW is an optimization scheme that assumes all of the isotropic elements of UHA has unity amplitude when calculation the beam pattern. In other words, beam pattern via UW (*i.e.* $w_H = 1$, $n \in [0, N_H - 1]$, where, w_H is UW amplitude and N_H is number of UHA elements) is performed at the expense of widening the main lobe. Because of this assumption, the beam pattern side lobes could be reduced. For a uniformly weighted array, the largest sidelobe is reduced to a certain level from the peak value. Moreover, in UW the nonuniformly weighted array can also be modified to UW in order to steer the beam to any direction desired and with suppressed sidelobe levels.

V. SIMULATION RESULTS ANALYSIS AND DESCRIPTIONS

The simulation results for the proposed scenario are based on the simulation settings listed in Table I below [54].

The simulation parameters illustrated in Table I and the MATLAB tool were used to run the simulation. Several numerical experiments are provided and compared to those

TABLE I. Simulation Parameters and Settings

Parameters	Value
Bandwidth (MHz)	8
Carrier Frequency (MHz)	617
Reuse Number	4
Temperature (K)	500
Number of Cells	19
Transmit Power (dBW)	10
Boltzmann's Constant (J/K)	1.3807×10^{-23}
Thermal Noise Power (dB)	-132.5806
Array Size	169
Element Spacing along X and Y	$\lambda/2$
Population Size	50
C1	2
C2	1.8
w	1
Number of Iterations	200

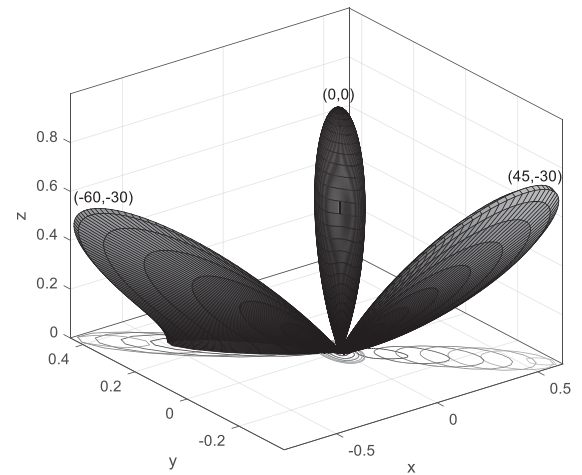


FIGURE 4. Beamsteered pattern and their respective contour of 169 elements of UHA at $(-60^\circ, -30^\circ)$, $(0^\circ, 0^\circ)$ and $(45^\circ, -30^\circ)$ angles.

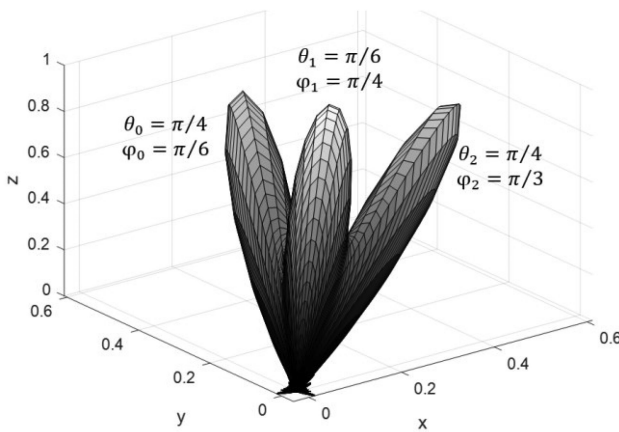


FIGURE 3. Three spots beam steered pattern created by a 169 elements UHA at different angles and same element spacing.

conducted using conventional PSO and UW. The experiments concern mainly with optimizing a 169-element UHA planar array. Fixed beams may be used in HAP communications networks that take advantage of the TVWS spectrum to generate spot beams to specific positions. Fig. 3 illustrates how the HAP beams are created as well as an illustration of a planar array that creates three spot beams. To achieve good communication coverage and signal quality, the three beams are each steered to a separate desired spot. The three beams are each guided to a different desirable spot to ensure good communication coverage and signal quality. As can be seen from Fig. 3, the beam steered for UHA is created at $(\frac{\pi}{4}, \frac{\pi}{6})$, $(\frac{\pi}{6}, \frac{\pi}{4})$ and $(\frac{\pi}{4}, \frac{\pi}{3})$.

Fig. 4 The spot beam steered and their respective contour is created by 169 elements of UHA at $(-60^\circ, -30^\circ)$, $(0^\circ, 0^\circ)$ and $(45^\circ, -30^\circ)$ angles and same element spacing. The figure furthermore, illustrated how beams are steered to a different desired location.

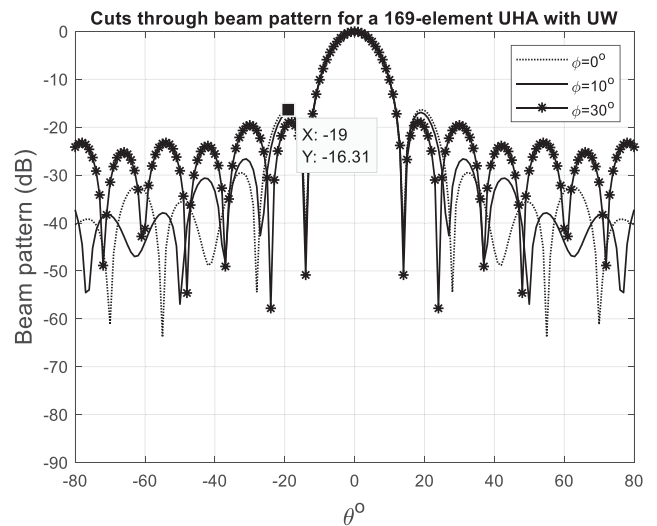


FIGURE 5. Cut plot of the beam pattern of UW scheme at different values of ϕ .

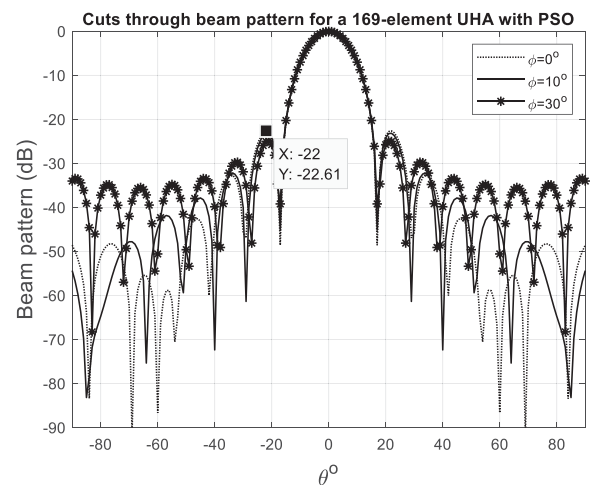


FIGURE 6. Cut plot of the beam pattern of PSO scheme at different values of ϕ .

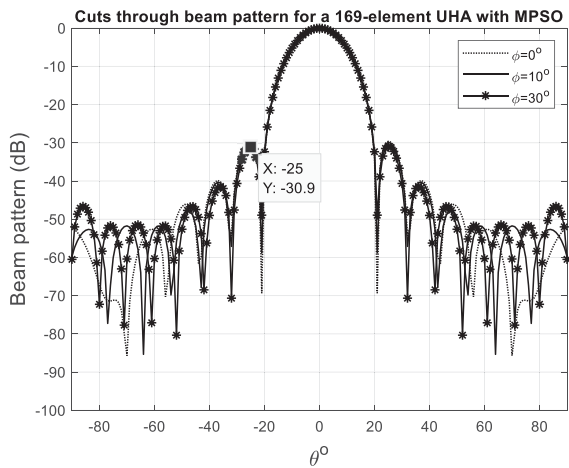


FIGURE 7. Cut plot of the beam pattern of proposed (MPSO) scheme at different values of ϕ .

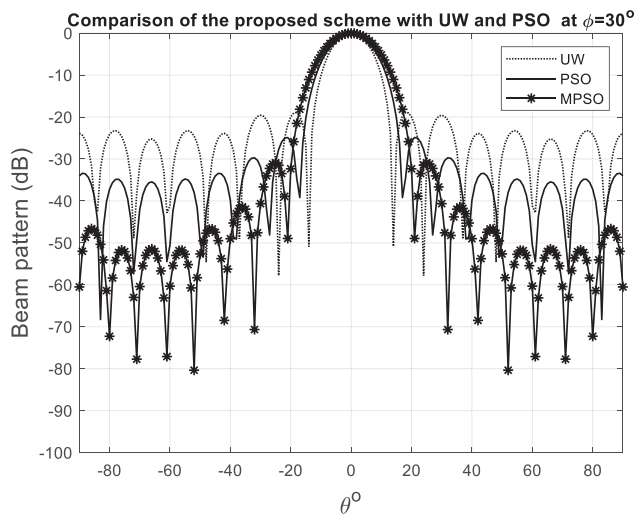


FIGURE 8. Beam pattern comparison of the proposed MPSO with UW and standard PSO at $\phi = 30^\circ$.

Fig. 5, 6, and 7 illustrated the cut plots of the beam pattern at different values of ϕ ($\phi = 0^\circ$, $\phi = 10^\circ$ and $\phi = 30^\circ$) using UW, PSO, and MPSO respectively. As can be seen from the cut plot the proposed model outperforms the other two schemes in reducing the SLL and optimizing the performance of the HAP wireless communication system by exploiting the TVWS spectrum.

As illustrated in Fig. 8, the proposed algorithm outperforms the Weighting and Standard PSO in improving the system performance of the HAP communication system using TVWS Spectrum. As expected, the sidelobe levels from the proposed algorithm are much lower and the main lobe is a bit wider in comparison to the UW and standard PSO. Table II demonstrates a novel type of beam pattern optimization algorithm MPSO compared with the UW and standard PSO taking into account the obtained directivity coefficient and maximum SLL with the same simulation parameters. As per the comparison, MPSO gave an optimized result.

TABLE II. Comparison of UW, PSO, and MPSO

Approach	SLL (dB)			θ	Gain
	$\phi = 0^\circ$	$\phi = 10^\circ$	$\phi = 30^\circ$		
UW	-16.31	-16.91	-19.03	19°	15
PSO	-22.77	-23.25	-24.89	21°	14.3
Proposed (MPSO)	-29.61	-29.91	-30.9	25°	14.3
Improvement compared with UW	13.3	13	11.87		
Improvement compared with PSO	6.84	6.66	6.01		

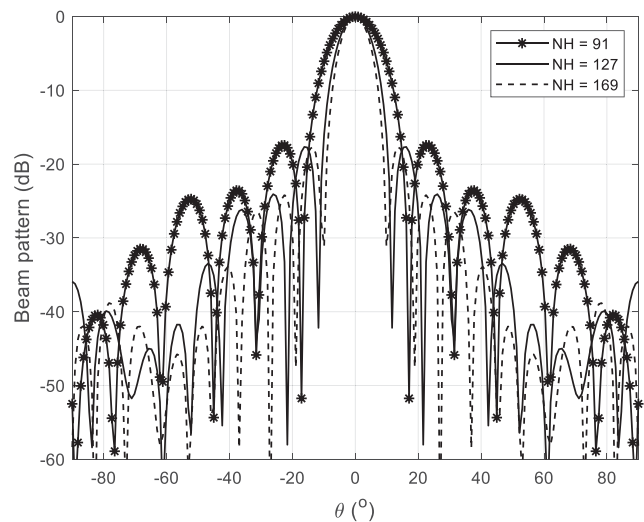


FIGURE 9. Beam pattern of 91, 127, and 169 elements of UHA.

The creation of the beam pattern for 91, 127, and 169 element UHA (NH) for the HAP wireless system employing the TVWS spectrum is displayed in Fig. 9. As can be seen in the diagram, as the number of elements rises, the beam gets more directed and the width of the sidelobe narrows. Instead of just broadcasting radio signals everywhere, the MPSO algorithm applied to UHA allows the beams to be directed or steer radio signals in a particular direction. As the number of elements of UHA (NH) increases, the beams became more directed since the radiated power is more concentrated to a certain targeted direction on account of the reduced beam width. The beam pattern for 169 elements of UHA became more directional and reduced SLL on account of narrower beamwidth than 97 and 127 UHA elements.

Figs. 10, 11, and 12 show the surface plots of the 169 element UHA's received power distribution for UW, conventional PSO, and MPSO, respectively. According to the comparison, MPSO outperforms the other schemes when it comes to upgrading HAP communication systems.

Fig. 13 depicts the surface plot of surface plots of the 169 element UHA's received power distribution for MPSO after the beam is steered to the desired location at $(-30^\circ, 60^\circ)$.

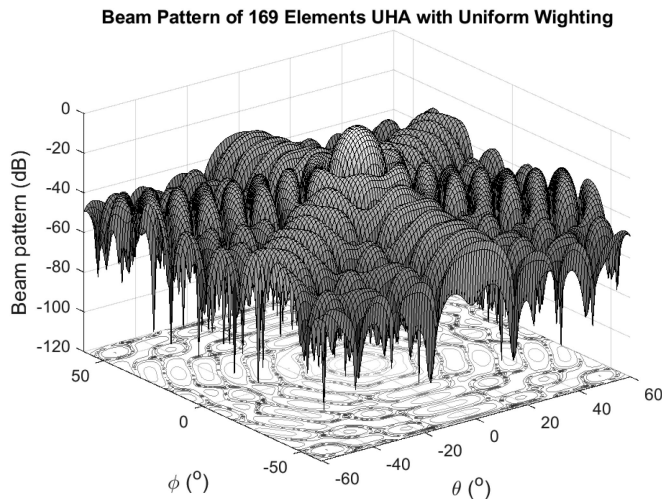


FIGURE 10. Surface plot of a uniformly excited UHA of 169 elements of isotropic elements with a UW beam pattern.

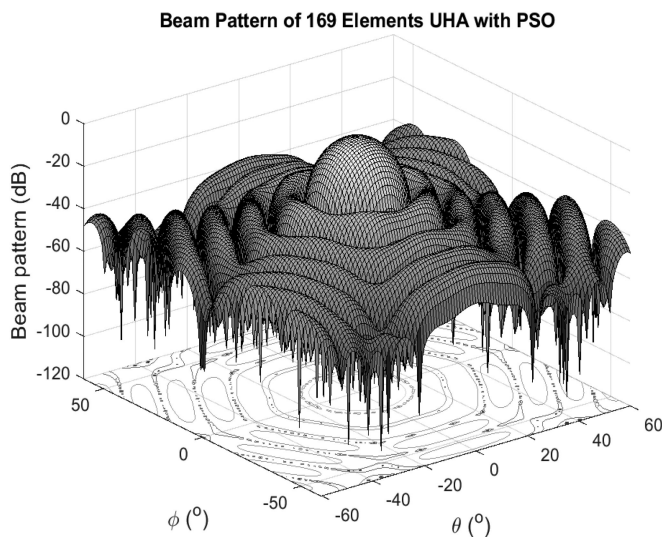


FIGURE 11. Surface plot of PSO-based beam pattern in a uniformly excited UHA of 169 isotropic elements.

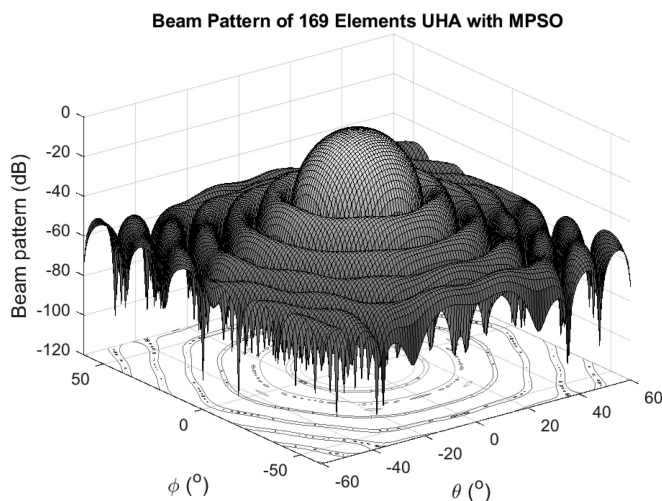


FIGURE 12. Surface plot of MPSO-based beam pattern of 169 isotropic elements in a uniformly excited UHA.

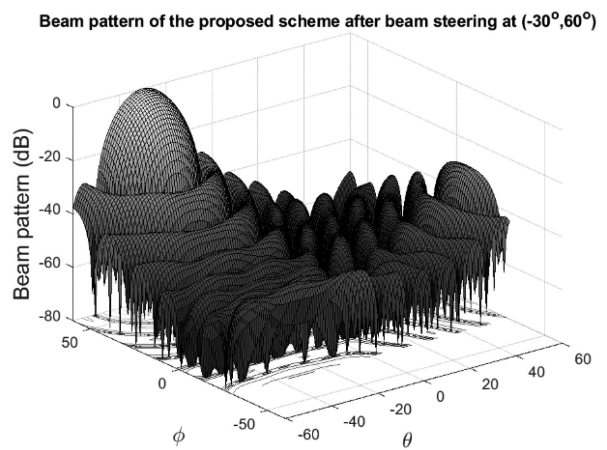


FIGURE 13. Beam steered at $(-30^\circ, 60^\circ)$ after applying MPSO scheme.

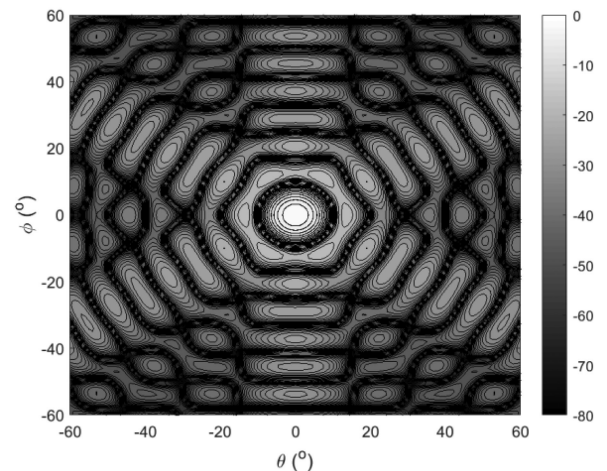


FIGURE 14. Contour plot of the received power distribution of a uniformly excited UHA of 169 elements of isotropic elements with UW.

Figs. 14, 15, and 16 show the contour plots of the 169 element UHA's received power distribution for UW, conventional PSO, and MPSO, respectively. According to the comparison, MPSO outperforms the other schemes when it comes to upgrading HAP communication systems.

Fig. 17 demonstrates the comparison of the average outage probability of 169 element UHA after applying UW, PSO, and MPSO. As per the comparison made in Fig. 17, the proposed algorithm gives the anticipated result with improved performance.

VI. CONCLUSION

This article demonstrates the possibility of exploiting TVWS spectrum band from the HAP for delivering a rural wireless broadband access through a steerable beam of UHA. The article is used the SINR based fitness parameter for population-based optimization algorithms in order to configure a planar UHA. The MPSO approach used produced a series of array weights. These weights were chosen to increase

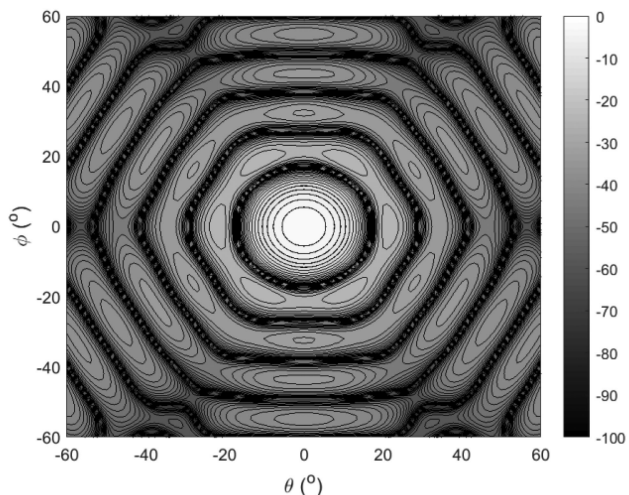


FIGURE 15. Contour plot of the received power distribution of a uniformly excited UHA of 169 elements of isotropic elements with PSO.

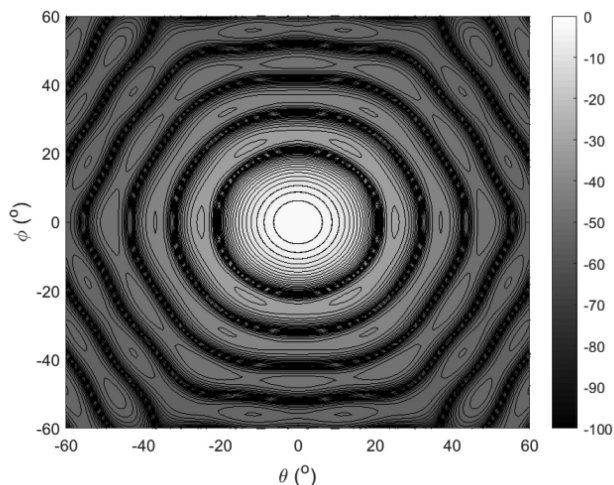


FIGURE 16. Contour plot of the received power distribution of a uniformly excited UHA of 169 elements of isotropic elements with MPSO.

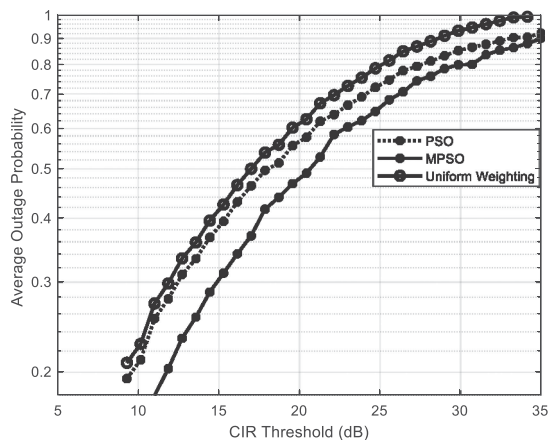


FIGURE 17. Average outage probability as a function of CIR threshold for 169 elements UHA.

power in the desired direction while reducing power in the direction of interferers. The findings reveal that the MPSO does better in terms of SLL reduction thereby improving CIR than a normal PSO. A comparison between PSO, UW, and MPSO, indicated that MPSO on average produces a lower amount of sidelobes, which is beneficial for avoiding interference. The computational results show that the UHA achieves a side-lobe level of -30.9 dB after applying MPSO which improves the sidelobe level by 6.01 dB and 11.87 dB compared with UW and PSO schemes with the cost of very small gain reduction at $\theta = 30^\circ$. The simulation findings show that the suggested optimization approach outperforms the other two schemes in improving the performance of the HAP communication system.

REFERENCES

- [1] CISCO, Annual Internet Report (2018–2023) White paper, Accessed: Jul. 2022. [Online]. Available: <https://www.cisco.com/c/en/us/solutions/collateral/executive-perspectives/annual-internet-report/white-paper-c11-741490.html>
- [2] International Telecommunications Union, “IMT traffic estimates for the years 2020 to 2030,” Electronic Publishing Geneva, Tech. Rep. M.2370, 2015.
- [3] J. Mitola and G. Q. Maguire, “Cognitive radio: Making software radios more personal,” *IEEE Pers. Commun.*, vol. 6, no. 4, pp. 13–18, Aug. 1999, doi: [10.1109/98.788210](https://doi.org/10.1109/98.788210).
- [4] J. Hoydis, S. ten Brink, and M. Debbah, “Massive MIMO in the UL/DL of cellular networks: How many antennas do we need?,” *IEEE J. Sel. Areas Commun.*, vol. 31, no. 2, pp. 160–171, Feb. 2013, doi: [10.1109/JSAC.2013.130205](https://doi.org/10.1109/JSAC.2013.130205).
- [5] B. Bengtsson and M. Ottersten, *Optimal and Suboptimal Transmit Beamforming*, 1st ed. Boca Raton, FL, USA: CRC Press, 2018.
- [6] G. M. Djuknic, J. Freidenfelds, and Y. Okunev, “Establishing wireless communications services via high-altitude aeronautical platforms: A concept whose time has come?,” *IEEE Commun. Mag.*, vol. 35, no. 9, pp. 128–135, Sep. 1997, doi: [10.1109/35.620534](https://doi.org/10.1109/35.620534).
- [7] S. Rajagopal, R. D. Roberts, and S. Lim, “IEEE 802.15.7 visible light communication: Modulation schemes and dimming support,” *IEEE Commun. Mag.*, vol. 50, no. 3, pp. 72–82, Mar. 2012, doi: [10.1109/MCOM.2012.6163585](https://doi.org/10.1109/MCOM.2012.6163585).
- [8] ITU, “ITU key 2005-2017 ICT data,” 2017. [Online]. Available: <https://www.Q5itu.int/en/ITU-D/Statistics/Pages/stat/default.aspx>
- [9] H. M. Hussien, K. Katzis, L. P. Mfupe, and E. T. Bekele, “Bridging the urban-rural broadband connectivity gap using 5G enabled HAPs communication exploiting TVWS spectrum,” *J. Eng. Res. Sci.*, vol. 1, no. 2, pp. 24–32, 2022.
- [10] S. Arum, D. Grace, and P. D. Mitchell, “A review of wireless communication using high-altitude platforms for extended coverage and capacity,” *Comput. Commun.*, vol. 157, pp. 232–256, 2020.
- [11] M. Giordani, M. Polese, M. Mezzavilla, S. Rangan, and M. Zorzi, “Toward 6G networks: Use cases and technologies,” *IEEE Commun. Mag.*, vol. 58, no. 3, pp. 55–61, Mar. 2020, doi: [10.1109/MCOM.001.1900411](https://doi.org/10.1109/MCOM.001.1900411).
- [12] L. Gavrilovska, V. Rakovic, and D. Denkovski, “From cloud RAN to open RAN,” *Wireless Pers. Commun.*, vol. 113, pp. 1–17, Mar. 2020.
- [13] K. Katzis, L. Mfupe, and H. M. Hussien, “Opportunities and challenges of bridging the digital divide using 5G enabled high altitude platforms and TVWS spectrum,” in *Proc. IEEE 8th Int. Conf. Commun. Netw.*, 2020, pp. 1–7, doi: [10.1109/ComNet47917.2020.9306090](https://doi.org/10.1109/ComNet47917.2020.9306090).
- [14] Z. Yang, A. Mohammed, and T. Hult, “Performance evaluation of WiMAX broadband from high altitude platform cellular system and terrestrial coexistence capability,” *J. Wireless Com Netw.*, vol. 2008, Art. no. 348626, doi: [10.1155/2008/348626](https://doi.org/10.1155/2008/348626).
- [15] J. Thornton, D. Grace, C. Spillard, T. Konefal, and T. C. Tozer, “Broadband communications from a high-altitude platform : The European HeliNet program,” *Electron. Commun. Eng. J.*, vol. 13, no. 3, pp. 138–144, Jun. 2001, doi: [10.1049/eej:20010304](https://doi.org/10.1049/eej:20010304).

- [16] S. G. Iskandar and M. E. Ernawan, "LTE uplink cellular capacity analysis in a high-altitude platforms (HAPS) communication," in *Proc. 11th Int. Conf. Telecommunication Syst., Serv., Appl.*, 2017, pp. 1–5.
- [17] M. Guan et al., "Efficiency evaluations based on artificial intelligence for 5G massive MIMO communication systems on high-altitude platform stations," *IEEE Trans. Ind. Inform.*, vol. 16, no. 10, pp. 6632–6640, Oct. 2020.
- [18] A. Chaoub et al., "6G for bridging the digital divide: Wireless connectivity to remote areas," *IEEE Wireless Commun.*, vol. 29, no. 1, pp. 160–168, Feb. 2022, doi: [10.1109/MWC.001.2100137](https://doi.org/10.1109/MWC.001.2100137).
- [19] S. Ananth, B. Wojtowicz, A. Cohen, N. Gulia, A. Bhattacharya, and B. Fox, "System design of the physical layer for Loon's high-altitude platform," *EURASIP J. Wireless Commun. Netw.*, vol. 2019, no. 1, 2019, Art. no. 170, doi: [10.1186/s13638-019-1461-x](https://doi.org/10.1186/s13638-019-1461-x).
- [20] J. Lun et al., *Solar Powered High Altitude Platform and Terrestrial Infrastructures*. York, U.K.: Univ. of York, 2017.
- [21] H. M. Hussien, K. Katzis, L. P. Mfupe, and E. T. Bekele., "A novel resource allocation for HAP wireless networks exploiting TVWS spectrum," in *Proc. IEEE AFRICON*, 2021, pp. 1–6, doi: [10.1109/AFRICON51333.2021.9570928](https://doi.org/10.1109/AFRICON51333.2021.9570928).
- [22] H. M. Hussien, K. Katzis, and L. P. Mfupe, "Dynamic spectrum allocation for TVWS wireless access from high altitude platform," in *Proc. Int. Conf. Elect., Comput. Energy Technol.*, 2021, pp. 1–6, doi: [10.1109/ICECET52533.2021.9698667](https://doi.org/10.1109/ICECET52533.2021.9698667).
- [23] H. M. Hussien, K. Katzis, and L. P. Mfupe, "Intelligent power allocation for cognitive HAP wireless networks using TVWS spectrum," in *Proc. Int. Conf. Elect., Comput. Energy Technol.*, 2021, pp. 1–6, doi: [10.1109/ICECET52533.2021.9698778](https://doi.org/10.1109/ICECET52533.2021.9698778).
- [24] A. W. See, O. Onireti, and M. A. Imran, "Will 5G see its blind side? Evolving 5G for universal internet access," in *Proc. Workshop Glob. Access Internet*, 2016, pp. 1–6, doi: [10.1145/2940157.2940158](https://doi.org/10.1145/2940157.2940158).
- [25] G. P. White and Y. V. Zakharov, "Data communications to trains from high-altitude platforms," *IEEE Trans. Veh. Technol.*, vol. 56, no. 4 II, pp. 2253–2266, 2007, doi: [10.1109/TVT.2007.897185](https://doi.org/10.1109/TVT.2007.897185).
- [26] S. Karapantazis and F. Pavlidou, "Broadband communications via high-altitude platforms: A survey," *IEEE Commun. Surv. Tuts.*, vol. 7, no. 1, pp. 2–31, Jan.–Mar. 2005, doi: [10.1109/COMST.2005.1423332](https://doi.org/10.1109/COMST.2005.1423332).
- [27] A. Mohammed and Z. Yang, "Broadband communications and applications from high altitude platforms," *Int. J. Recent Trends Eng.*, vol. 1, no. 3, pp. 239–243, 2009.
- [28] A. Mohammed and T. Hult, "Capacity evaluation of a high altitude platform diversity system equipped with compact MIMO antennas," *ACEEE Int. J. Commun.*, vol. 1, no. 1, pp. 1–4, 2010.
- [29] F. A. Dicanidia and S. Genovesi, "Spectral efficiency improvement of 5G massive MIMO systems for high-altitude platform stations by using triangular lattice arrays," *Sensors*, vol. 21, no. 9, Art. no. 3202, 2021, doi: [10.3390/s21093202](https://doi.org/10.3390/s21093202).
- [30] Z. Xu, G. White, and Y. Zakharov, "Optimisation of beam pattern of high-altitude platform antenna using conventional beamforming," *IEEE Proc.-Commun.*, vol. 153, 2006, Art. no. 865, doi: [10.1049/ip-com:20050355](https://doi.org/10.1049/ip-com:20050355).
- [31] G. M. Djuknic, J. Freidenfelds, and Y. Okunev, "Establishing wireless communications services via high-altitude aeronautical platforms: A concept whose time has come?," *IEEE Commun. Mag.*, vol. 35, no. 9, pp. 128–135, Sep. 1997, doi: [10.1109/35.620534](https://doi.org/10.1109/35.620534).
- [32] M. Chrysomallis, "Smart antennas," *IEEE Antennas Propag. Mag.*, vol. 42, no. 3, pp. 129–136, Jun. 2000, doi: [10.1109/74.848965](https://doi.org/10.1109/74.848965).
- [33] C. Christodoulou and C. A. Balanis, "Uniform circular arrays for smart antennas," *IEEE Antennas Propag. Mag.*, vol. 47, no. 4, pp. 192–206, Aug. 2005.
- [34] R. Bera, R. Lanjewar, D. Mandal, R. Kar, and S. Prasad, "Comparative study of circular and hexagonal antenna array synthesis using improved particle swarm optimization," *Procedia - Procedia Comput. Sci.*, vol. 45, pp. 651–660, 2015, doi: [10.1016/j.procs.2015.03.126](https://doi.org/10.1016/j.procs.2015.03.126).
- [35] M. Dessouky, H. Sharshar, and Y. Albagory, "Efficient sidelobe reduction technique for small-sized concentric circular arrays," *Prog. Electromagn. Res.*, vol. 65, pp. 187–200, 2006.
- [36] L. C. Kretly, A. S. Cerqueira, and A. Tavora, "A hexagonal adaptive antenna array concept for wireless communication applications," in *Proc. 13th IEEE Int. Symp. Pers., Indoor Mobile Radio Commun.*, 2002, pp. 247–249, doi: [10.1109/PIMRC.2002.1046698](https://doi.org/10.1109/PIMRC.2002.1046698).
- [37] J. Thornton, D. Grace, M. H. Capstick, and T. C. Tozer, "Optimizing an array of antennas for cellular coverage from a high altitude platform," *IEEE Trans. Wireless Commun.*, vol. 2, no. 3, pp. 484–492, May 2003, doi: [10.1109/TWC.2003.811052](https://doi.org/10.1109/TWC.2003.811052).
- [38] J. Thornton and D. Grace, "Effect of antenna aperture field on co-channel interference, capacity and payload mass in high altitude platform communications," *ETRI J.*, vol. 26, pp. 467–474, 2004, doi: [10.4218/etrij.04.0104.0008](https://doi.org/10.4218/etrij.04.0104.0008).
- [39] A. H. Naqvi and S. Lim, "Review of recent phased arrays for millimeter-wave wireless communication," *Sensors*, vol. 18, 2018, Art. no. 3194, doi: [10.3390/s18103194](https://doi.org/10.3390/s18103194).
- [40] K. Kibaroglu, M. Sayginer, T. Phelps, and G. M. Rebeiz, "A 64-element 28-GHz phased-array transceiver with 52-dBm EIRP and 8–12-Gb/s 5G link at 300 meters without any calibration," *IEEE Trans. Microw. Theory Techn.*, vol. 66, no. 12, pp. 5796–5811, Dec. 2018, doi: [10.1109/TMTT.2018.2854174](https://doi.org/10.1109/TMTT.2018.2854174).
- [41] R. N. Cai, M. C. Yang, X. Q. Zhang, M. Li, and X. F. Liu, "A novel multi-beam lens antenna for high altitude platform communications," in *Proc. IEEE 75th Veh. Technol. Conf.*, 2012, pp. 1–5, doi: [10.1109/VETECS.2012.6239876](https://doi.org/10.1109/VETECS.2012.6239876).
- [42] M. Stoneback and K. Madsen, "A planar all-silicon 256-element Ka-band phased array for high-altitude platforms (HAPs) application," in *Proc. IEEE/MTT-S Int. Microw. Symp.*, 2018, pp. 783–786, doi: [10.1109/MWSYM.2018.8439632](https://doi.org/10.1109/MWSYM.2018.8439632).
- [43] F. Enache, D. Depărețeanu, and F. Popescu, "Optimal design of circular antenna array using genetic algorithms," in *Proc. 9th Int. Conf. Electron., Comput. Artif. Intell.*, 2017, pp. 1–6, doi: [10.1109/ECAI.2017.8166392](https://doi.org/10.1109/ECAI.2017.8166392).
- [44] D. Mandal, S. P. Ghoshal, and A. K. Bhattacharjee, "Optimized radii and excitations with concentric circular antenna array for maximum sidelobe level reduction using wavelet mutation-based particle swarm optimization techniques," *Telecommun. Syst.*, vol. 52, pp. 2015–2025, 2013, doi: [10.1007/s11235-011-9482-8](https://doi.org/10.1007/s11235-011-9482-8).
- [45] G. Sun, Y. Liu, Z. Chen, Y. Zhang, A. Wang, and S. Liang, "Thinning of concentric circular antenna arrays using improved discrete cuckoo search algorithm," in *Proc. IEEE Wireless Commun. Netw. Conf.*, 2017, pp. 1–6, doi: [10.1109/WCNC.2017.7925959](https://doi.org/10.1109/WCNC.2017.7925959).
- [46] A. M. Ismaiel, E. Elsaidy, Y. Albagory, H. A. Atallah, A. B. Abdel-Rahman, and T. Sallam, "Performance improvement of high altitude platform using concentric circular antenna array based on particle swarm optimization," *Int. J. Electron. Commun.*, vol. 91, pp. 85–90, 2018, doi: [10.1016/j.aueu.2018.05.002](https://doi.org/10.1016/j.aueu.2018.05.002).
- [47] Ó. Quevedo-Teruel, S. Member, and E. Rajo-Iglesias, "Ant colony optimization in thinned array synthesis with minimum sidelobe level," *IEEE Antennas Wireless Propag. Lett.*, vol. 5, pp. 349–352, 2006, doi: [10.1109/LAWP.2006.880693](https://doi.org/10.1109/LAWP.2006.880693).
- [48] J. Kennedy and R. C. Eberhard, "Particle swarm optimization," in *Proc. Int. Conf. Neural Netw.*, 1995, pp. 1942–1948.
- [49] A. M. M. and H. M. Elragal, "Department, antenna array pattern synthesis and wide null control using enhanced particle swarm optimization," *Prog. Electromagn. Res.*, vol. 17, pp. 1–14, 2009.
- [50] J. Litva and T. K.-Y. Lo, *Digital Beamforming in Wireless Communications*. Norwood, MA, USA: Artech House, 1996.
- [51] F. Gross, *Smart Antennas for Wireless Communications*, 1st ed. New York, NY, USA: McGraw-Hill, 2005.
- [52] R. T. Compton, *Adaptive Antennas: Concepts and Performance*. Englewood Cliffs, NJ, USA: Prentice-Hall, 1988.
- [53] W. H. Tranter et al., *Principles of Communication Systems Simulation with Wireless Applications*, 1st ed. Englewood Cliffs, NJ, USA: Prentice Hall, 2003.
- [54] H. M. Hussien, K. Katzis, L. P. Mfupe, and E. T. Bekele, "Capacity, coverage and power profile performance evaluation of a novel rural broadband services exploiting TVWS from high altitude platform," *IEEE Open J. Comput. Soc.*, vol. 3, pp. 86–95, 2022, doi: [10.1109/OJCS.2022.3183158](https://doi.org/10.1109/OJCS.2022.3183158).

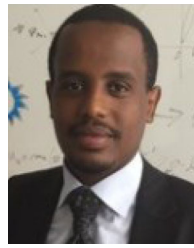


HABIB MOHAMMED HUSSEIN received the bachelor's degree from Adama Science and Technology University, Addis Ababa, Ethiopia, in 2008, and the M.Sc. degree in electrical and electronic engineering (signal and information processing technology) from Tianjin University, Tianjin, China, in 2012. He is currently working toward the Ph.D. degree with Adis Abau Institute of Technology, Addis Ababa University, Addis, Ethiopia. His current research interests include high altitude platform, handoff schemes, TV white space technology, radio resource allocation and optimization, call admission control, heterogenous network coexistence issues, and 5G IoT.



KONSTANTINOS KATZIS (Senior Member, IEEE) received the B.Eng. degree in computer systems engineering and the M.Sc. degree in radio systems engineering from the University of Hull, Hull, U.K., in 2000 and 2001 respectively, and the Ph.D. degree in electronics from the University of York, York, U.K. He is currently an Associate Professor with European University Cyprus, Engomi, Cyprus. His current research interests include dynamic spectrum access and cognitive radio, architectures for 5G and beyond, and

wireless communications from aerial platforms. He has also been working toward the development of highly efficient resource allocation techniques and handoff techniques optimised for the operation of high-altitude platform communication systems. His work involved modeling of the platform movements and simulating the effects on the communications. He currently holds the position of the Secretary in IEEE1900.6 standard and he is also a MC member of COST action CA20120 (Intelligence-Enabling Radio Communications for Seamless Inclusive Interactions - INTERACT). Recently, he has been awarded with the Fulbright Visiting Scholar fund for his proposal “Requirement Analysis of 5G Networks Supporting IoT-Health Applications” in collaboration with the Information Technology Laboratory , National Institute of Standards & Technology, Washington DC, USA.



EPHREM TESHALE BEKELE (Senior Member, IEEE) received the B.Sc. degree in electrical engineering from Bahir Dar University, Bahir Dar, Ethiopia, in 2007, the M.Sc. degree in telecommunications engineering and the Ph.D. degree in information and communications technology from the University of Trento, Trento, Italy, in 2011, and 2015, respectively. From 2007 to 2009, he was an Assistant Lecturer with Bahir Dar University. He is currently an Assistant Professor with the Addis Ababa Institute of Technology (AAiT), Addis

Ababa University, Addis Ababa, Ethiopia, and an Associate Faculty Member of the ELEDIA Research Center. He is also a Visiting Lecturer with Bahir Dar University, and a Member of the Applied Electromagnetic Research Group, AAiT. His main research interests include electromagnetic nondestructive testing, technology “domestication,” and RF regulation.



LUZANGO PANGANI MFUPE (Senior Member, IEEE) received the bachelor’s, master’s, and Ph.D. degrees in electrical engineering from the Tshwane University of Technology, Pretoria, South Africa. He is an experienced Principal Research Scientist, Innovator, and Entrepreneur with demonstrated leadership in large and cutting-edge technology projects. technically skilled in dynamic spectrum management (DSM), experienced in television white spaces (TVWS), defense and civilian spectrum sharing models, formulation of spectrum

regulations and policies, development of geo-location spectrum databases, advanced wireless networks design and modeling, satellite communications, airborne wireless networks (AWNs), artificial intelligence/machine learning for future wireless communications, such as 5G, computer simulations, lecturing, supervision, and SMMEs support.